Cancer Cell
Article

Pharmacological Inhibition of BMK1 Suppresses Tumor Growth through Promyelocytic Leukemia Protein

Qingkai Yang,[1,7] Xianming Deng,[5,7] Bingwen Lu,[2,7] Michael Cameron,[6] Colleen Fearns,[3] Matthew P. Patricelli,[4] John R. Yates, III,[2,*] Nathanael S. Gray,[5,*] and Jiing-Dwan Lee[1,*]
[1]Department of Immunology and Microbial Science
[2]Department of Chemical Physiology
[3]Department of Chemistry
The Scripps Research Institute, 10550 North Torrey Pines Road, La Jolla, CA 92037, USA
[4]ActivX Biosciences, 11025 North Torrey Pines Road, La Jolla, CA 92037, USA
[5]Dana Farber Cancer Institute, Harvard Medical School, 250 Longwood Avenue, Boston, MA 02115, USA
[6]Translational Research Institute-Drug Metabolism and Pharmacokinetics, Scripps Florida, 130 Scripps Way, Jupiter, FL 33458, USA
[7]These authors contributed equally to this work
*Correspondence: jyates@scripps.edu (J.R.Y.), nathanael_gray@dfci.harvard.edu (N.S.G.), jdlee@scripps.edu (J.-D.L.)
DOI 10.1016/j.ccr.2010.08.008

SUMMARY

BMK1 is activated by mitogens and oncogenic signals and, thus, is strongly implicated in tumorigenesis. We found that BMK1 interacted with promyelocytic leukemia protein (PML), and inhibited its tumor-suppressor function through phosphorylation. Furthermore, activated BMK1 notably inhibited PML-dependent activation of p21. To further investigate the BMK-mediated inhibition of the tumor suppressor activity of PML in tumor cells, we developed a small-molecule inhibitor of the kinase activity of BMK1, XMD8-92. Inhibition of BMK1 by XMD8-92 blocked tumor cell proliferation in vitro and significantly inhibited tumor growth in vivo by 95%, demonstrating the efficacy and tolerability of BMK1-targeted cancer treatment in animals.

INTRODUCTION

Four MAP kinase pathways exist in mammalian cells: ERK1/2, JNK, p38, and BMK1 (Chang and Karin, 2001; Johnson and Lapadat, 2002; Pearson et al., 2001; Raman et al., 2007). BMK1 is most similar to ERK1/2 because both contain the Thr-Glu-Tyr dual phosphorylation motif. However, unlike ERK1/2, BMK1 has a unique activating loop structure and an uncommonly large C-terminal nonkinase domain. The C-terminal half of BMK1 contains a nuclear localization signal (NLS) that is critical for nuclear localization of BMK1 (Lee et al., 1995). The ERK1/2 and BMK1 cascades are both activated by mitogens and by oncogenic signals and, thus, are strongly implicated in tumorigenesis (Chang and Karin, 2001; Johnson and Lapadat, 2002; Kato et al., 1997, 1998; Pearson et al., 2001). Specifically, deregulated BMK1 signaling has been associated with properties of human malignancies including chemoresistance of breast tumor cells (Weldon et al., 2002), uncontrolled proliferation of ErbB2-overexpressing carcinomas (Esparis-Ogando et al., 2002), metastatic potential of prostate tumor cells (Mehta et al., 2003), and tumor-associated angiogenesis (Hayashi et al., 2005).

Three sequentially activated kinases make up the central core of the MAP kinase module: a MAP kinase kinase kinase, or MEKK; a MAP kinase kinase, or MEK; and a MAP kinase. The signaling core in the BMK1 pathway consists of the kinases, MEKK2/MEKK3, MEK5, and BMK1 (Hayashi and Lee, 2004). MEK5 is the only known direct upstream regulatory kinase of BMK1 (Kato et al., 1997). However, MEK5 can be inhibited by inhibitors of MEK1/2 (Kamakura et al., 1999; Mody et al., 2001), such as PD98059 and U0126, which have been considered as specific inhibitors of the ERK1/2 pathway. As such, experimental results produced using these two inhibitors need

Significance

The BMK1/ERK5 pathway is the last discovered and the least studied mammalian MAP kinase cascade. Herein, we describe the development of the small-molecule inhibitor for BMK1 that is effective not only in cells but also in animals. Using this inhibitor, we determined that BMK1 inhibits the tumor suppressor activity of cellular PML, and more importantly, we demonstrated the efficacy and tolerability of BMK1-targeted cancer treatment in animals. As BMK1 is expressed in most, if not all, tumor cells, our results suggest that cancer therapies targeting BMK1 will have broad application for treating diverse types of human tumors.

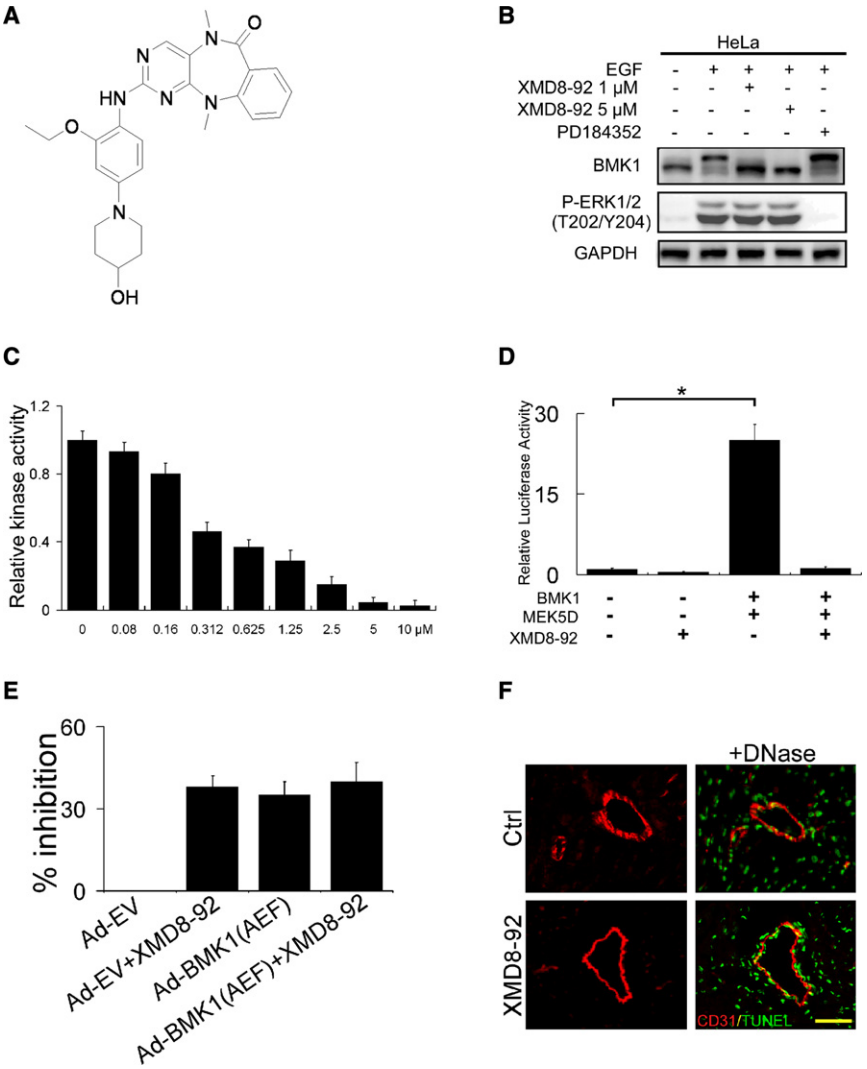

Figure 1. Development of a Pharmacological Inhibitor of BMK1

(A) Chemical structure of XMD8-92.

(B) HeLa cells were serum starved overnight followed by treatment with 1 or 5 μM XMD8-92 or 1 μM PD184352 as indicated for 1 hr. Cells were then stimulated with EGF for 17 min and BMK1 activation was detected by mobility retardation (Abe et al., 1996). ERK1/2 activation was detected by an antiphospho-ERK1/2 (T202/Y204) antibody.

(C) HEK293 cells were cotransfected with expression plasmids of MEK5D and BMK1. After 48 hr, BMK1 was immunoprecipitated and in vitro kinase assays were carried out in the presence of the indicated amount of XMD8-92. The ATP concentration was measured by the Kinase-Glo Luminescent Kinase Assay Platform. Kinase activity is expressed relative to the kinase activity in cells without XMD8-92 treatment, which was taken as 1. n = 3, ± standard error of mean (SEM).

(D) Expression plasmids of MEK5D and BMK1 were transfected into HEK293 as indicated. After 36 hr, these cells were cotransfected with vectors for pCMV-β and the reporter plasmid pG5ElbLuc along with a GAL4 fusion expression vector containing MEF2C for 3 hr and then treated with 5 μM XMD8-92 for a further 16 hr. The luciferase activities were normalized against cells transfected with pG5ElbLuc and pGAL4 reporter plasmid alone, whose value was taken as 1. n = 3, ± SEM, *p < 0.01.

(E) HeLa cells were infected with Ad-EV or Ad-BMK1(AEF), as indicated, 24 hr before treatment with or without XMD8-92 (5 μM) for 48 hr, followed by MTT assays. % growth inhibition = (1 − MTT value of cells in each experimental group/MTT value of cells treated with Ad-EV only) × 100. n = 3, ± SEM.

(F) Immunofluorescent analysis of CD31 (red) and TUNEL (green) in heart sections from control and XMD8-92 treated. DNase treatments were used as positive controls for TUNEL staining. Scale bar represents 100 μm. n = 6 mice, n = 10 slices.

See also Figure S1 and Tables S1–S5.

to be re-evaluated using more specific inhibitors of the BMK1 and the ERK1/2 cascades. So far, there is no specific small-molecule inhibitor of BMK1 that is effective both in cells and animals. More importantly, the lack of this kind of BMK1 inhibitor has hampered the understanding of the physiological/pathological roles of BMK1 through cellular and animal studies.

RESULTS

Development of Pharmacological Inhibitors of BMK1

During the course of developing isoform-selective polo kinase inhibitors, we synthesized a library of analogs of the highly selective, adenosine triphosphate (ATP)-competitive polo kinase inhibitor, BI-2536 (Steegmaier et al., 2007). By screening a subset of the library against a diverse panel of 402 kinases, we were able to explore the full range of potential kinase targets of this class of compounds (Goldstein et al., 2008). We discovered that expansion of the 6-membered aliphatic ring of BI-2536 to a 7-membered ring containing an anthranilic acid resulted in loss of polo kinase inhibition activity but serendipitously resulted in compounds that exhibited high selectivity toward BMK1. Structure-activity guided optimization based on the ability of the compounds to inhibit cellular BMK1 autophosphorylation stimulated by EGF (Kato et al., 1998) in conjunction with kinase selectivity analysis resulted in the synthesis of XMD8-92 (Figure 1A). The kinase selectivity of XMD8-92 was determined by profiling the inhibitor at a concentration of 10 μM against a panel of 402 diverse kinases using an in vitro ATP-site competition binding assay (Fabian et al., 2005; Karaman et al., 2008). Kinases that exhibited >90% displacement by XMD8-92 were determined to be BMK1, DCAMKL1, DCAMKL2, TNK1, and PLK4. XMD8-92 exhibited the greatest affinity toward BMK1 with a measured dissociation constant (K_D) of 80 nM, while DCAMKL2, TNK1, and PLK4 exhibited K_Ds of 190, 890, and 600 nM, respectively (see Table S1 available online). This represents a remarkable level of selectivity considering the very large number of kinases that have been assayed. Moreover, XMD8-92 was profiled against all detectable kinases in HeLa cell lysates using the

KiNativ method (Patricelli et al., 2007) and was found to be about 10-fold more selective for BMK1 with a IC_{50} of 1.5 μM than the most potent off-targets, TNK1 (IC_{50} = 10 μM) and ACK1 (also known as TNK2, IC_{50} = 18 μM). Other weak off-targets included the kinase domain 2 of RSK1 and RSK2, PIK4A and PIK4B, and FAK (Table S2). Notably, MEK5 was not significantly inhibited by XMD8-92 at up to 50 μM. There is also no significant inhibitory effect of XMD8-92 on TNK1 and PLK4 detected in vitro and in vivo (Figure S1). The BMK1 potency and selectivity determined by the KiNativ method support the conclusion that the anticancer effects of XMD8-92 detailed herein are due to inhibition of BMK1.

We tested the effect of XMD8-92 on the cellular activity of BMK1. Growth factor-induced activation of cellular BMK1, but not the structurally similar ERK1/2, was effectively blocked by 1 μM XMD8-92 (Figure 1B), while PD184352, an ERK1/2 inhibitor, only blocked ERK1/2 but not BMK1 activation by EGF (Figure 1B). XMD8-92 also significantly reduced BMK1 activity in in vitro kinase assays (Figure 1C). In addition, *trans*-reporter assays showed that XMD8-92 dramatically reduced the BMK1-dependent transactivating activity of MEF2C, a known substrate for BMK1 (Kato et al., 1997) (Figure 1D).

As the BMK1 pathway is critical for cell proliferation (Kato et al., 1998), we next tested whether XMD8-92, through its specific ability to block BMK1 activity, has an antiproliferative effect on cells. The extent of inhibition by XMD8-92 in HeLa cells is indistinguishable from that by dominant negative BMK1, BMK1(Ala-Glu-Phe [AEF]), administered through infection with recombinant adenovirus encoding BMK1(AEF), Ad-BMK1(AEF) (Figure 1E). The inhibitory effect of XMD8-92 on proliferation was observed in a wide variety of cancer cell lines (Figure S2). Moreover, additional treatment of Ad-BMK1(AEF)-infected HeLa cells with XMD8-92 did not have a further inhibitory effect when compared to cancer cells treated with XMD8-92 alone (Figure 1E), indicating that at least some of the antiproliferative capacity of XMD8-92 is through inhibition of the activity of BMK1.

Subsequently, to assess the utility of XMD8-92 in animal experiments, we analyzed the pharmacokinetics and tolerability of XMD8-92. The pharmacokinetics of XMD8-92 was evaluated in Sprague-Dawley rats given a single intravenous or oral dose. XMD8-92 was found to have a 2.0 hr half-life clearance of 26 mL/min/kg. The compound had moderate tissue distribution with a calculated volume of distribution of 3.4 L/kg. XMD8-92 had high oral bioavailability with 69% of the dose absorbed. After a single oral dose of 2 mg/kg, maximal plasma concentrations of approximately 500 nM were observed by 30 min, with 34 nM remaining 8 hr postdose (Figure S1). In tolerability experiments (Tables S3, S4, and S5), high plasma concentrations of drug (~10 μM after intraperitoneal [IP] dosing of 50 mg/kg) were maintained throughout the 14 days. The drug appeared to be well tolerated and the mice appeared healthy with no sign of distress. No vasculature instability was observed in the XMD8-92-treated mice (Figure 1F; Tables S4 and S5). Together, these results demonstrated that XMD8-92 is an effective and specific inhibitor of BMK1 in vitro and in vivo.

BMK1 Is in Complex with PML and Suppresses Its Anticancer Activity

To study the molecular mechanism by which BMK1 regulates cell proliferation, we carried out mass spectrometry (MS) analysis of cellular BMK1-interacting proteins and revealed that BMK1 interacted with promyelocytic leukemia protein (PML) (Table S6). Western blot analysis using two different anti-PML antibodies showed that PML coprecipitated with BMK1 (Figure 2A) and that reciprocal immunoprecipitation of PML using anti-PML antibody brought down cellular BMK1 (Figure 2B). These data indicate that endogenous BMK1 is in complex with PML.

As PML is a tumor suppressor and known to regulate cell proliferation, we next tested whether BMK1 controls the antitumor function of PML. We found that p21, one of the downstream effectors of PML and a key modulator of cell proliferation (Bernardi and Pandolfi, 2007; Salomoni and Pandolfi, 2002), was significantly induced when the expression level of BMK1 was suppressed by siRNA (Figure 2C). Inhibition of BMK1 activation by XMD8-92 also significantly induced p21 expression in cells (Figure 2D), and its induction was substantially reduced in PML null cells (Figure 2D). Using PML-knockdown cell lines, we also demonstrated that PML and p21 are involved in XMD8-92-mediated suppression of cancer cell proliferation (Figure S2). These results indicated that BMK1 not only is in complex with PML but also suppresses the expression of the cell-cycle regulator p21, through inhibiting the antitumor function of PML.

BMK1 Suppress PML Function through Phosphorylation

Since BMK1 is known to regulate the activity of cellular proteins through phosphorylation (Hayashi et al., 2001; Kato et al., 1997; Kato et al., 2000), we carried out an in vitro kinase assay using activated BMK1 kinase and recombinant PML as substrate, followed by mass spectrometry analysis (details in Experimental Procedures) to map the potential phosphorylation sites on PML by BMK1. We identified that S403 and T409 of PML as potential phosphorylation sites (Figure 3A). Mutation of these two sites to alanine significantly inhibited the phosphorylation of PML by BMK1 in an in vitro kinase assay (Figure 3B) indicating these two sites in PML are major phosphorylation sites by the BMK1 kinase. PML phosphorylation by BMK1 in vivo was also demonstrated (Figure S3). We next mutated S403 and T409 to aspartic acid (PML-2D) to mimic the phosphorylation of PML by BMK1. We found that recombinant adenovirus-mediated expression of PML2D (S403D/T409D) in PML-deficient cells did not significantly restore their responsiveness to XMD8-92-dependent p21 induction unlike wild-type PML, which did restore responsiveness (Figure 3C). As PML is known to modulate p21 through p53 (Guo et al., 2000), the role of BMK1 on p53 regulation is still not clear (Figure S4). These results indicate that BMK1 suppresses PML function through phosphorylation of S403 and T409 of PML (Figure 3C).

Activated BMK1 Translocates from the Cytosol to Colocalize with PML in the Nucleus

It has been shown that, on activation, BMK1 translocates from the cytoplasm to the nucleus (Kondoh et al., 2006; Yan et al., 2001). As PML is known to localize to the PML-nuclear body (PML-NB), through which it mediates diverse cellular functions, we wondered whether BMK1, after activation, could move to the nucleus and colocalize with PML in PML-NBs. We expressed a dominant negative form of MEK5, MEK5A (Kato et al., 1997), to inhibit the activation of BMK1 in cells (Figure 4, first-row panels). Conversely, we expressed a dominant active form of MEK5,

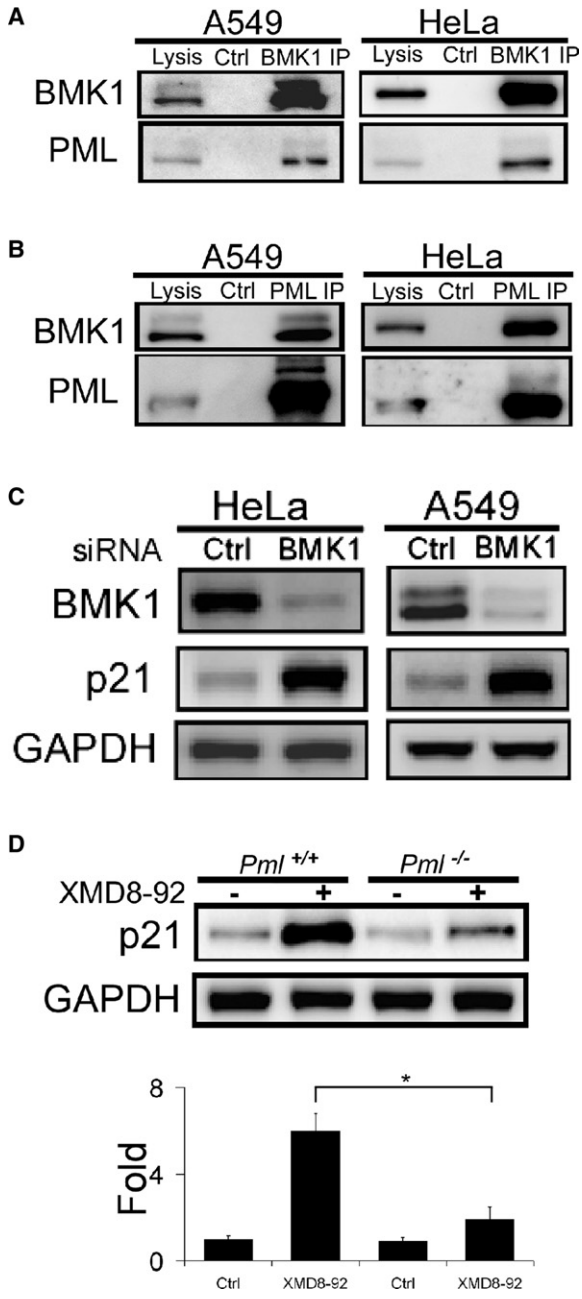

Figure 2. BMK1 is in Complex with PML and Suppresses the Anticancer Function of PML in Tumor Cells

(A) Cellular BMK1 was immunoprecipitated from cell lysates from A549 and HeLa cells with anti-BMK1 antibody or rabbit IgG, as control. The resultant immunoprecipitates and total cell lysates were then tested for the presence of PML using anti-PML antibody.

(B) Endogenous PML was immunoprecipitated from cell lysates of A549 and HeLa cells with anti-PML antibody or rabbit IgG, as control. The existence of BMK1 in these immunoprecipitates was analyzed using western blots as described in (A).

(C) HeLa and A549 cells were transfected with control or BMK1-specific siRNA. Cell lysates were analyzed by western blot using anti-p21 or anti-GAPDH antibodies as noted. n = 3, ± standard error of mean (SEM), *p < 0.01.

(D) $Pml^{+/+}$ MEF and $Pml^{-/-}$ MEF cells were treated with or without XMD8-92 (5 μM) for 16 hr as indicated. Cell lysates were analyzed by western blot using anti-p21 antibody. The levels of p21 protein expression were quantified by densitometry and normalized against GAPDH. The amount of the p21 protein in the $Pml^{+/+}$ MEF without XMD8-92 treatment was taken as 1. n = 5, ± SEM, *p < 0.01.

See also Figure S2 and Table S6.

MEK5D, to keep BMK1 activated in cells (Figure 4A, second-row panels). With increased expression of PML in cells, activated BMK1 is colocalized with PML in the PML-NBs (Figure 4A, fourth-row panels) whereas nonactivated BMK1 stays in the cytoplasm (Figure 4A, third-row panels). BMK1 contains a kinase domain in its N-terminal half and a nonkinase domain in its C-terminal half (Figure 4B). We next tested the involvement of these two domains in the colocalization of activated BMK1 and PML in PML-NBs. We demonstrate that the kinase region, but not the nonkinase region, of BMK1 is sufficient for the colocalization of BMK1 and PML in PML-NBs (Figure 4B). This result indicates that BMK1, on activation, translocates from the cytosol to the nucleus and, through its kinase domain, colocalizes with PML in PML-NBs (Figure 5).

BMK1 Is a Potential Drug Target for Treating Cancer

To evaluate the effectiveness of XMD8-92 in inhibiting the activity of BMK1 in tumors, we tested the compound in mice xenografted with human tumors. XMD8-92 was found to effectively inhibit BMK1 activation as well as induce PML's downstream effector, p21 (Figure 6A). More importantly, treatment of the mice with XMD8-92 1 day, several days, or weeks after inoculation of the tumor cells all significantly inhibit the growth of the xenografted human or syngeneic mouse tumors (Figure 6B), without obvious side effects to the animals. Immunostaining of tumor sections showed that XMD8-92 effectively inhibited the incorporation of BrdU during tumor cell division (Figure 6C) indicating XMD8-92 blocks tumor cell proliferation, one of the anticancer effects of PML. As both BMK1 and PML are involved in angiogenesis (Bernardi et al., 2006; Borden and Culjkovic, 2009; Hayashi et al., 2004, 2005), we tested whether XMD8-92 blocks angiogenesis in vivo and found that XMD8-92 significantly inhibits basic fibroblast growth factor (bFGF) induced angiogenesis in Matrigel plugs (Figure 6D). These results indicated that XMD8-92 exerts its antitumor effect by blocking tumor cell proliferation and tumor-associated angiogenesis, and, possibly, through other BMK1-dependent mechanisms yet to be tested or discovered.

We further examined whether the antitumor effect of XMD8-92 is specific to its anti-BMK1 capacity. The extent of tumor growth inhibition by XMD8-92 is identical to that elicited using dominant negative BMK1 administered through intratumoral injection of Ad-BMK1(AEF) (Figure 7A). Importantly, the additional treatment of Ad-BMK1(AEF) did not have a further inhibitory effect on the tumor-bearing mice treated with XMD8-92 alone (Figure 7A) indicating the antitumor capacity of XMD8-92 is, at least partly, through blocking the activity of BMK1.

We next evaluate the role of PML in XMD8-92-dependent inhibition of tumor growth. We found that depleting PML in tumor cells significantly lowered, but did not completely abrogate, the inhibitory effect of XMD8-92 on their growth in mice (Figure 7B). As XMD8-92 inhibits tumor cell proliferation and neovascularization (Figures 6C and 6D), the reason why PML depletion in tumor cells can only partly reverse the antitumor effect of

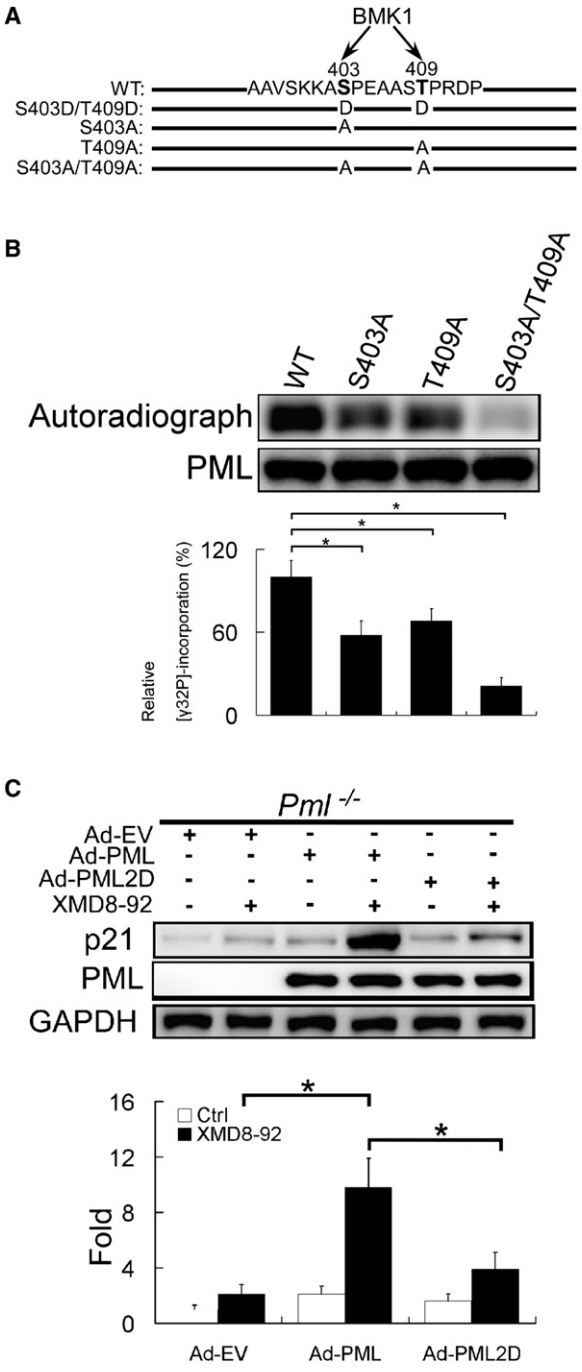

Figure 3. BMK1 Regulates PML Function through Phosphorylation

(A) A schematic representation of wild-type and mutant PMLs. The amino acid sequences of potential BMK1 phosphorylation sites in PML are indicated.

(B) Mutation of potential BMK1 sites in full-length PML reduces phosphorylation by BMK1. Equal amounts of full-length wild-type or mutant recombinant PMLs were subjected to in vitro BMK1-mediated phosphorylation assay of PML in the presence of activated recombinant BMK1. The levels of relative [γ^{32}P]-incorporation in PML or PML mutants were quantified by densitometry and normalized against the loading amount of PML or PML mutants in each reaction mix, respectively. The value of relative [γ^{32}P]-incorporation of the wild-type PML by BMK1 was taken as 100%. n = 3, ± standard error of mean (SEM), *p < 0.01.

(C) *Pml*$^{-/-}$ MEF cells were infected with Ad-EV, Ad-PML or Ad-PML2D as indicated. Three days later, these cells were treated with or without XMD8-92 (5 μM) for 16 hr as noted. The expression levels of p21 were quantified as described in Figure 2D except that the amount of the p21 protein in the Ad-EV-infected *Pml*$^{-/-}$ cells without XMD8-92 treatment was taken as 1. n = 3, ± SEM, *p < 0.01.

See also Figure S3.

XMD8-92 may be that PML in tumor cells is responsible only for mediating XMD8-92-mediated growth arrest of cancer cells and not for XMD8-92-dependent angiogenesis inhibition. Moreover, increasing the expression level of wild-type PML in these PML-knockdown (KD) tumor cells restored their sensitivity to XMD8-92-mediated inhibition of tumor growth (Figure 7B). In contrast, expression of PML2D in the PML-KD cells did not re-establish their responsiveness to XMD8-92-mediated suppression of tumor proliferation (Figure 7B). These data indicate that PML plays a role in XMD8-92-mediated suppression of tumor growth.

Taken together, these results demonstrated that the BMK1 pathway in animals can be blocked effectively by a small-molecule inhibitor without apparent adverse effects and, more importantly, BMK1 inhibition is a very effective way to prevent cancer development in animals.

DISCUSSION

The promyelocytic leukemia protein PML (also called MYL, RNF71, PP8675, or TRIM19) has been implicated in the regulation of a range of cellular functions, such as inhibition of proliferation, induction of cellular senescence and apoptosis, as well as maintenance of genomic stability (Bernardi and Pandolfi, 2007). It is well known that compromising PML anticancer function by gene translocation (to produce the PML-RAR fusion protein) leads to acute promyelocytic leukemia. PML-RAR fusion protein not only represses PML function but also represses transcriptional activity mediated by RAR-RXR, thereby disrupting retinoid signaling (Altucci and Gronemeyer, 2001). Although the physiological roles of PML are not yet fully understood, the tumor-suppressive function of PML is generally recognized (Bernardi et al., 2006; Salomoni and Pandolfi, 2002; Trotman et al., 2006). One of the critical anticancer/antiproliferative functions of PML is through activation of the tumor suppressor, p21, through transcriptional regulation of p53 (Bernardi and Pandolfi, 2007; Bernardi et al., 2004; Fogal et al., 2000; Guo et al., 2000; Pearson et al., 2000; Pearson and Pelicci, 2001). Previous reports have described the regulation of PML through phosphorylation by kinases such as ERK1/2 and CK2 (Hayakawa and Privalsky, 2004; Scaglioni et al., 2006). Herein, we report that the mitogenic MAP kinase, BMK1, interacts with PML and suppresses its antitumor actions such as p21 activation. However, the effect of BMK1 on p53 regulation is not clear (Figure S4) and needs further investigation. Because BMK1 negatively regulates PML tumor suppressor function and BMK1 is activated by a variety of deregulated oncogenes (e.g., Her2, Ras, and STAT3), it is likely that the oncogene-induced BMK1 activation increases the proliferation/survival/chemoresistance potential of tumor cells by dampening the anticancer capacity of PML.

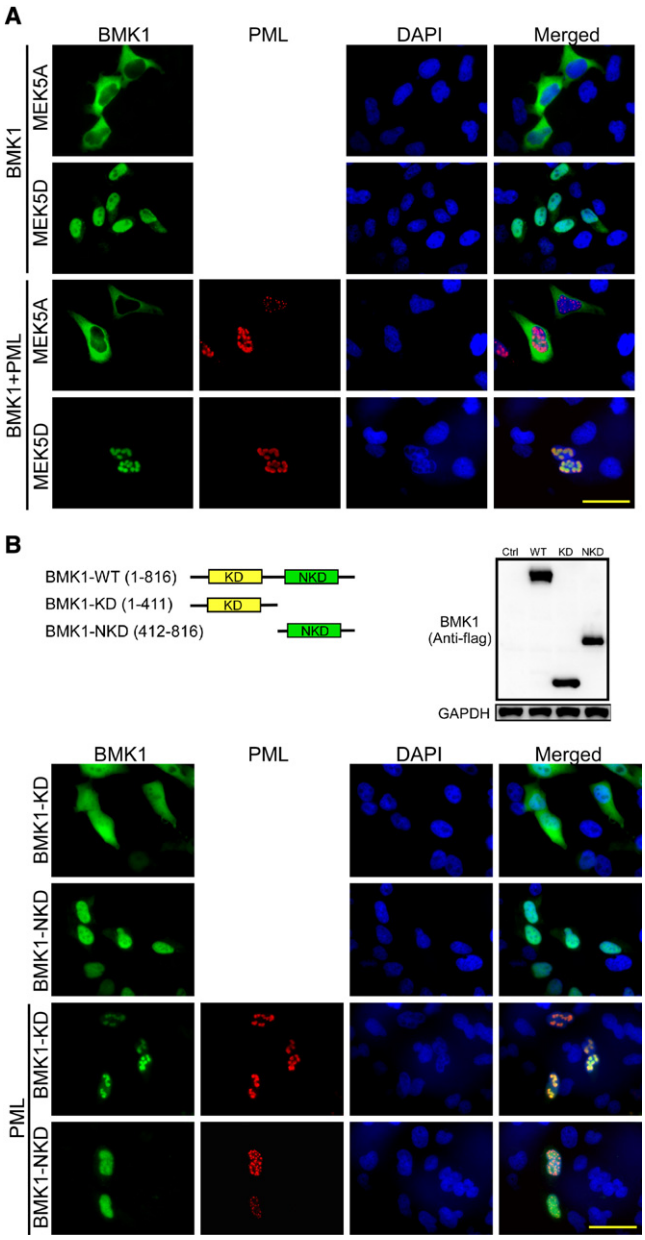

Figure 4. Activated BMK1 Translocates from the Cytosol to Colocalize with PML in the Nucleus

(A) Fluorescent microscopy images of HeLa cells transfected with expression vectors encoding BMK1, PML, MEK5A, or MEK5D, as indicated. These cells were stained with anti-BMK1 (green, first-column panels) or with anti-PML (PG-M3) antibody (red, second-column panels) as noted. Nuclei were shown by DAPI staining (blue, third-column panels). Merged images (yellow, fourth-column panels). n = 5. Scale bar represents 10 μm.

(B) Fluorescent microscopy images of HeLa cells transfected with expression vectors encoding the N-terminal kinase domain of BMK1 (BMK1-KD), the C-terminal nonkinase domain of BMK1 (BMK1-NKD) and/or PML, as indicated. These cells were stained with anti-BMK1 (green, first-column panels) or with anti-PML (PG-M3) antibody (red, second-column panels) as noted. Nuclei were shown by DAPI staining (blue, third-column panels). Merged images (yellow, fourth-column panels). n = 5. Scale bar represents 10 μm. See also Figure S4.

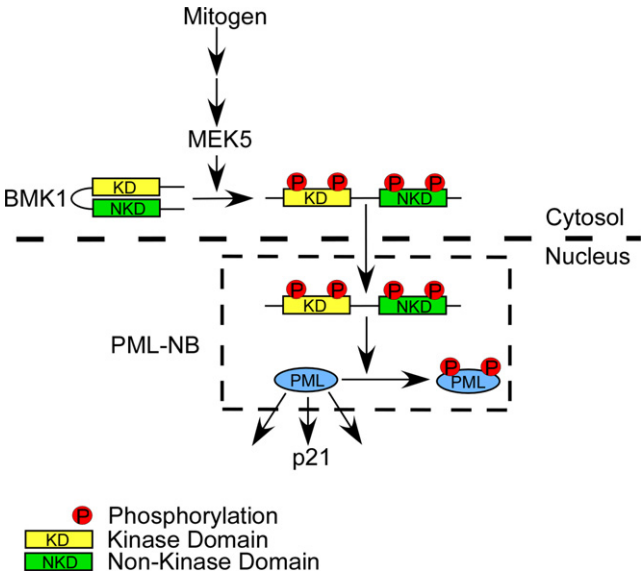

Figure 5. Scheme for PML Regulation by BMK1

BMK1 promotes tumor development not only by inhibiting the PML tumor suppressor described herein but also by supporting tumor angiogenesis (Hayashi et al., 2005; Hayashi and Lee, 2004; Pi et al., 2005), tumor metastasis (Sawhney et al., 2009; Sticht et al., 2008; Zhou et al., 2008) and chemo-resistance of tumor cells (Weldon et al., 2002). In addition, no significant feed-back compensatory activation of any other signaling pathway was detected, so far, by blocking the BMK1 pathway using XMD8-92 (Figure S4). Conditional knockout of BMK1 in various tissues of mice (e.g., in cardiomyocytes, neurons, hepatocytes, and T and B cells) has no obvious effect on the development, behavior, reproduction and aging of the animals (Hayashi and Lee, 2004), suggesting that BMK1 should be an attractive target for pharmaceutical intervention in cancer therapy. However, the instability of the vasculature observed in mice depleted of endothelial BMK1 (Hayashi et al., 2004) has discouraged the therapeutic development of a BMK1 inhibitor. Compared to BMK1 knockout, which is much more severe as it leads to complete and irreversible annihilation of BMK1 gene product in the tissues targeted, pharmaceutical inhibition of BMK1 only targets the kinase activity of the enzyme. Therefore, we believe that applying the BMK1 inhibitor in animals should have no or little unfavorable effect on vascular integrity. Indeed, we have demonstrated that XMD8-92 is a very effective ATP-competitive inhibitor that inhibits BMK1 activity in animals and reduces tumor growth by 95% without inducing vasculature abnormalities (Figure 1F; Tables S4 and S5). These results strengthen the notion that blocking the BMK1 pathway may be an effective approach for treating human cancer.

EXPERIMENTAL PROCEDURES

KiNativ Profiling Method

KiNativ profiling of XMD8-92 was carried out with both an ATP and adenosine diphosphate (ADP) acylphosphate-desthiobiotin as described previously (Patricelli et al., 2007) with the following modifications. HeLa cell lysates

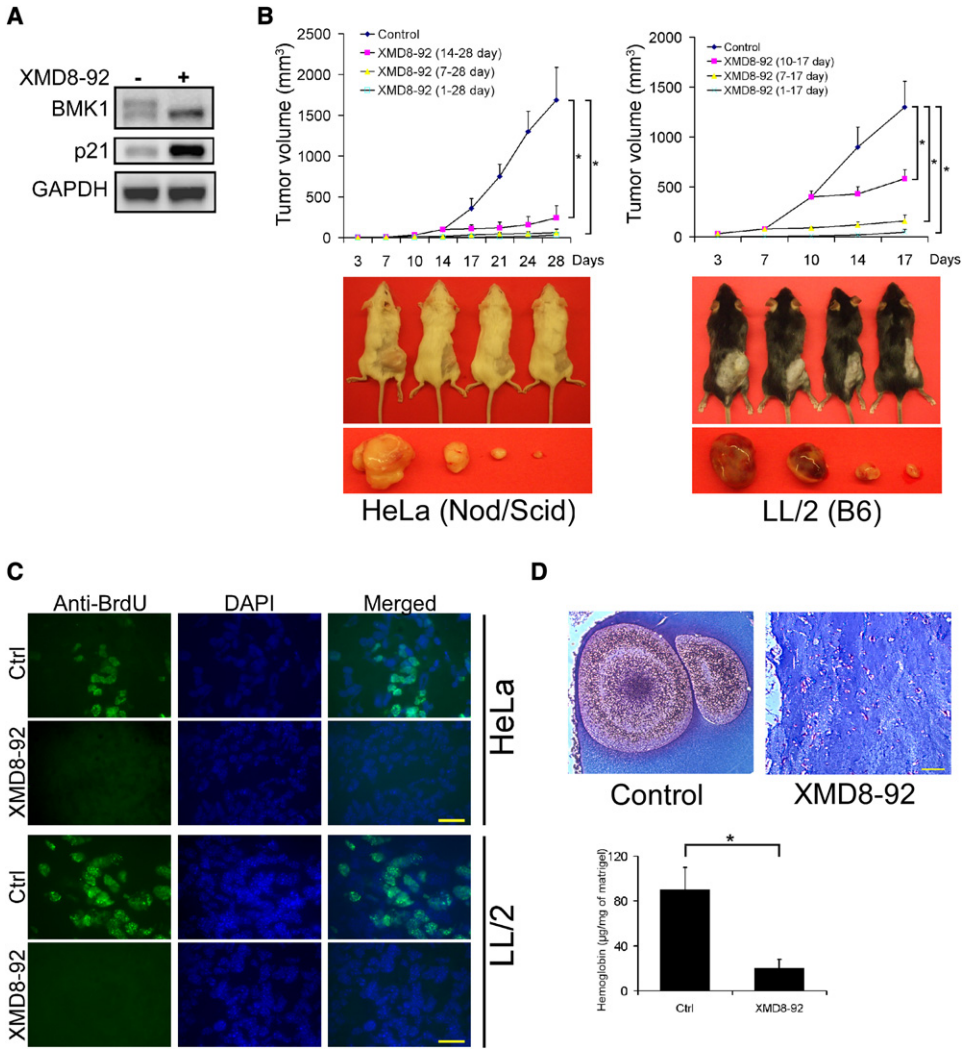

Figure 6. BMK1 Is a Potential Drug Target for Treating Cancer

(A) A549 cells were injected subcutaneously into the flanks of NOD/SCID mice. After 3 weeks, these tumor-bearing mice were injected intraperitoneally with XMD8-92 or vehicle for 2 days. The XMD8-92 concentration in these tumors were analyzed and shown in the Supplemental Information (see also Figure S5). The tumor homogenates were used to detect both BMK1 activity and p21 expression using western blot as described in Figure 2D.

(B) Mouse xenograft models were established as described in Experimental Procedures. (Top panels) Starting 1 day or at the indicated time after injection of the human (HeLa) or mouse (LL/2) tumor cells, XMD8-92 was administered twice daily and the tumor growth in these mice was measured every 2 or 3 days. (Lower panels) Representative mice from each group (control mice on the left) showing the growth of xenograft tumors at the end of an experiment. n = 6 mice, ± standard error of mean (SEM), *$p < 0.01$.

(C) Fluorescence microscopy images of HeLa or LL/2 tumor sections from XMD8-92 treated or control mice as indicated. The sections were stained with anti-BrdU antibody or DAPI as noted. n = 6 mice, n = 9 slices. Scale bar represents 10 μm.

(D) Mice were implanted with Matrigel containing 400 ng/mL bFGF. The next day, mice were treated with XMD8-92 or vehicle for 6 days. The Matrigel plugs were then harvested, sectioned and stained with Masson's trichrome (n = 6 mice, n = 9 slices.). Hemoglobin content in the Matrigel plugs was assessed as described (Hayashi et al., 2005). n = 6 mice, ± SEM, *$p < 0.01$. Scale bar represents 100 μm.

(5 mg/mL total protein) were incubated in the presence of XMD8-92 at 50 μM, 10 μM, 2 μM, 0.8 μM, and 0 μM for 15 min before addition of the ATP or ADP acylphosphate probe (5 μM final probe concentration). All reactions were carried out in duplicate. Probe reactions proceeded for 10 min and the reaction stopped by the addition of urea and processed for MS analysis as described (Patricelli et al., 2007). Samples were analyzed by LC-MS/MS on a linear ion trap mass spectrometer using a time segmented "target list" designed to collect MS/MS spectra from all kinase peptide-probe conjugates that can be detected in HeLa cell lysates. This target list was generated and validated by prior exhaustive analysis of HeLa lysates. Up to four characteristic fragment ions for each kinase peptide-probe conjugate were used to extract signals for each kinase, and a comparison of inhibitor treated to control (untreated) lysates allowed for precise determination of % inhibition at each point. A manuscript describing the details of this targeted mass spectrometry approach is in preparation.

Cell Culture, Stable Isotope Labeling with Amino Acid in Cell Culture Labeling, and Sample Preparation for MS

GIBCO SILAC DMEM basal cell culture medium (Invitrogen, Carlsbad, CA) containing 2 mM L-glutamine, 10% dialyzed fetal bovine serum (FBS)

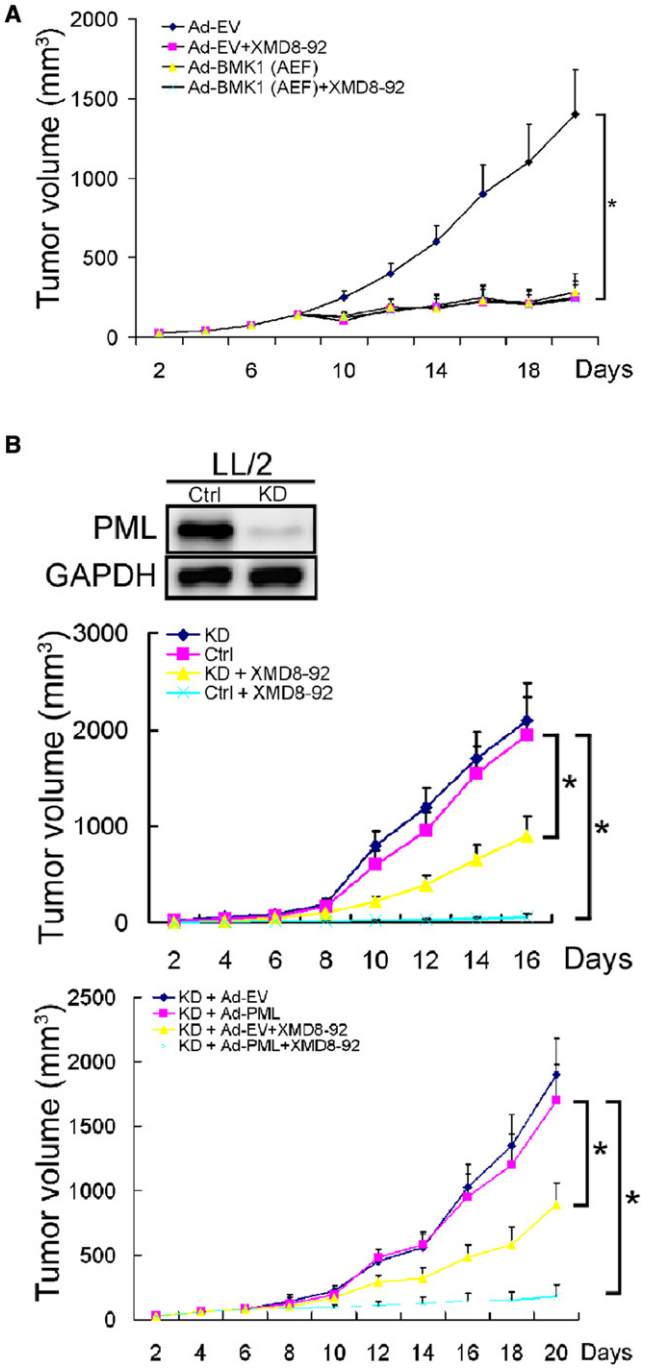

Figure 7. Pharmacological Inhibition of BMK1 Suppresses Tumor Growth through PML

(A) Mouse tumor model with syngeneic LL/2 carcinoma was established as described in Experimental Procedures. Starting 7 days after injection of LL/2 tumor cells into mice, the mice were treated with intratumoral injection of recombinant adenovirus encoding BMK1(AEF) [Ad-BMK1(AEF)] or empty vector control (Ad-EV) as indicated. One day after starting the injection of recombinant adenoviruses, XMD8-92 was administered to the indicated mice. n = 6 mice, ± standard error of mean (SEM), *p < 0.01.

(B) Mouse tumor models with PML-knockdown (PML-KD) and control LL/2 carcinoma (Ctrl) were established (middle panel) similar to syngeneic LL/2 tumor model. Starting 7 days after injection of the LL/2 tumor cells, the mice were treated with XMD8-92 or vehicle for another 9 days as described in (A). (Bottom panel) Mice bearing PML-KD LL/2 tumors for 7 days were injected with recombinant adenovirus encoding wild-type PML [Ad-PML], mutant PML [Ad-PML2D], or empty vector control [Ad-EV] intratumorally. One day after starting the injection of recombinant adenoviruses, XMD8-92 or vehicle was administered to the indicated mice. n = 6 mice, ± SEM, *p < 0.01.

(Invitrogen), and 100 U/ml penicillin and streptomycin was supplemented with 100 mg/l L-lysine and 20 mg/l L-arginine or 100 mg/L [U-$^{13}C_6$]-L-lysine and 20 mg/L [U-$^{13}C_6$, $^{15}N_4$]-L-arginine (Invitrogen) to make the "Light" SILAC or "Heavy" SILAC culture media, respectively. HeLa cells were obtained from ATCC and were propagated in SILAC medium for more than nine generations to ensure nearly 100% incorporation of labeled amino acids before the experiment was performed. After being washed with precooled PBS buffer, HeLa cells were lysed in E1A (250 mM NaCl, 50 mM HEPES (pH 7.5), 0.1% NP40, 5 mM EDTA, protease inhibitor cocktail (Roche, Indianapolis, IN) and phosphatase inhibitor cocktail (Roche) or RIPA (1× PBS, 1% NP40, 0.5% sodium deoxycholate, 0.1% SDS, 0.1 mg/ml PMSF, 1 mM sodium orthovanadate, protease inhibitor cocktail (Roche) and phosphatase inhibitor cocktail (Roche) lysis buffer, respectively. Light cell lysate and Heavy lysate were mixed at a 1:1 ratio, and the mixed lysates were incubated with the precipitating antibody for 8 hr, followed by 16 hr incubation with protein G beads (Invitrogen). Immune complexes were washed three times in lysis buffer (E1A or RIPA, respectively) and once in sterile water, and then incubated in 8 M urea for 30 min at room temperature. The supernatant was reduced with DTT, and then alkylated with iodoacetamide. The resulting samples from E1A or RIPA lysis buffer were dialyzed against 2 M urea/100 mM NH_4HCO_3 at 37°C for 5 hr and then analyzed by multidimensional liquid chromatography coupled with tandem mass spectrometry (MudPIT) twice. Because the existence of the stable (heavy) isotope in nature is <1%, any "light" peptide detected by MudPIT with no similar amount of "heavy" peptide detected was considered as a contaminant.

In Vivo Tumorigenesis Experiments

The following animal handling and procedures were approved by the Scripps Institutional Animal Care and Use Committee and followed the National Institutes of Health guidelines.

HeLa Xenograft Model

HeLa cells (5 × 10^5) were resuspended in DMEM and injected subcutaneously (SC) into the right flank of 6-week-old NOD/SCID mice (day 0). On the second day (day 1) after tumor cell injection, mice were randomized into two groups (6 animals [XMD8-92 (1–28 days)] and 18 animals [control]). The XMD8-92 (1–28 days) group was treated with XMD8-92 at the dose of 50 mg/kg twice a day IP. The control group received daily injections of the carrier solution as control. On the day 7, the control group was randomized into two groups (6 animals [XMD8-92 (7–28 days)] and 12 animals [control]). On day 14, the remaining control group was randomized into two groups (six animals [XMD8-92 (14–28 days)] and six animals [control]). Treatment with XMD8-92 in XMD8-92 (7–28 days) and XMD8-92 (14–28 days) groups was initiated on day 7 and day 14, respectively. Tumor size was measured using a caliper, and tumor volume was determined by using the formula: L × W^2 × 0.52, where L is the longest diameter and W is the shortest diameter.

LL/2 Xenograft Model

LL/2 cells (1 × 10^6) were resuspended in DMEM and injected SC into the right flank of 6-week-old C57Bl/6 mice (day 0). On the second day (day 1) after tumor cell injection, mice were randomized into two groups (6 animals [XMD8-92 (1–17 days)] and 18 animals [control]). The XMD8-92 (1–17 days) group was treated with XMD8-92 at the dose of 50 mg/kg twice a day intraperitoneally. The control group received daily injections of the carrier solution as control. On the day 7, the control group was randomized into two groups (6 animals [XMD8-92 (7–17 days)] and 12 animals [control]). And on the day 14, the remaining control group was randomized into two groups (six animals [XMD8-92 (10–17 days)] and six animals [control]). Treatment with XMD8-92 in XMD8-92 (7–17 days) and XMD8-92 (10–17 days) groups was initiated on day 7 and day 10, respectively.

Recombinant Adenovirus Treatment

LL/2 cells (1 × 10^6) were injected SC into C57Bl/6 mice (day 0). Recombinant adenoviral particles were generated as described in our previous study

(Hayashi et al., 2001). On the day 7, mice were randomized into four groups [Ad-EV, Ad-BMK1(AEF), Ad-EV+XMD8-92, and Ad-BMK1(AEF)+XMD8-92] (six animals per group). Mice were injected intratumorally (IT) with either empty adenovirus (Ad-EV) or recombinant adenovirus encoding BMK1(AEF) [Ad-BMK1(AEF)] on day 7, day 11, day 15, day 19, using the procedure previously described (Kim et al., 2004). Ad-EV+XMD8-92 and Ad-BMK1 (AEF)+XMD8-92 groups were treated with XMD8-92 from day 8 to day 20 using the procedure described in the LL/2 xenograft model. The other two groups [Ad-EV and Ad-BMK1(AEF)] received injections of the carrier solution instead as control.

PML Reconstitution

PML shRNAi knockdown and control cell lines were built using pGIPZ-shRNA-mir-PML (Lentiviral) and pGIPZ (Lentiviral) plasmids from Openbiosystems (Huntsville, AL). Knockdown (1×10^6) (48 animals) or control (12 animals) LL/2 cells were injected SC into C57Bl/6 mice (day 0). On the second day (day 1) after tumor cell injection, mice were randomized into 10 groups (six animals per group) [KD, Ctrl, KD+XMD8-92 and Ctrl+XMD8-92; KD+Ad-EV, KD+Ad-PML, KD+Ad-PML2D(S403D/T409D), KD+Ad-EV+XMD8-92, KD+Ad-PML+XMD8-92, and KD+Ad-PML2D(S403D/T409D)+XMD8-92]. The KD+XMD8-92 and Ctrl+XMD8-92 groups were treated with XMD8-92 at the dose of 50 mg/kg twice a day IP for 16 days. The KD and Ctrl groups received daily injections of the carrier solution as control for 16 days. The KD+Ad-EV, KD+Ad-PML, KD+Ad-PML2D, KD+Ad-EV+XMD8-92, KD+Ad-PML+XMD8-92, and KD+Ad-PML2D+XMD8-92 groups were injected IT with either empty adenovirus (Ad-EV), Ad-PML, or Ad-PML2D recombinant adenovirus encoding PML or PML2D on day 7, day 11, day 15, day 19, using the procedure previously described (Kim et al., 2004). KD+Ad-EV+XMD8-92, KD+Ad-PML+XMD8-92, and KD+Ad-PML2D+XMD8-92 groups were treated with XMD8-92 from day 8 to day 20 using the procedure described in the LL/2 xenograft model. The KD+Ad-EV and KD+Ad-PML and KD+Ad-PML2D groups received injections of the carrier solution instead as control.

A549 Xenograft Model

To ascertain that XMD8-92 can block BMK1 in vivo, 1×10^6 A549 cells, whose endogenous BMK1 autophosphorylation was detectable by western blotting, were resuspended in DMEM and injected SC into the right flank of 6-week-old NOD/SCID mice. On the 21st day after the injection, mice were randomized into two groups (two animals per group). One group was treated with XMD8-92 at the dose of 50 mg/kg twice a day. The other group was treated with the carrier solution as control. After 2 days, the A549 tumor was homogenized in E1A buffer followed by western blot analysis.

The effectiveness of BMK1 inhibition in xenograft tumors was shown in the Supplemental Information (Figure S5).

Statistical Analysis

p values were calculated with the Student's t test.

SUPPLEMENTAL INFORMATION

Supplemental Information includes five figures and six tables and can be found with this article online at doi:10.1016/j.ccr.2010.08.008.

ACKNOWLEDGMENTS

We thank Dr. G. Blandino, Dr. M. Kim, and Dr. P.P. Pandolfi for the PML null and control cell lines. We also thank Ambit Biosciences for performing the KinomeScan kinase selectivity profiling. This work was supported by the National Institutes of Health (CA079871 and CA114059 to J.-D.L) and by funds from the Tobacco-Related Disease, Research Program of the University of California, 15RT-0104 (J.-D.L.). The Gray lab receives funding from Novartis. M.P.P. is an employee of ActivX Biosciences, Inc., a wholly owned subsidiary of Kyorin Pharmaceuticals.

Received: December 17, 2009
Revised: June 1, 2010
Accepted: July 21, 2010
Published: September 13, 2010

REFERENCES

Abe, J., Kusuhara, M., Ulevitch, R.J., Berk, B.C., and Lee, J.D. (1996). Big mitogen-activated protein kinase 1 (BMK1) is a redox-sensitive kinase. J. Biol. Chem. *271*, 16586–16590.

Altucci, L., and Gronemeyer, H. (2001). The promise of retinoids to fight against cancer. Nat. Rev. Cancer *1*, 181–193.

Bernardi, R., and Pandolfi, P.P. (2007). Structure, dynamics and functions of promyelocytic leukaemia nuclear bodies. Nat. Rev. Mol. Cell Biol. *8*, 1006–1016.

Bernardi, R., Scaglioni, P.P., Bergmann, S., Horn, H.F., Vousden, K.H., and Pandolfi, P.P. (2004). PML regulates p53 stability by sequestering Mdm2 to the nucleolus. Nat. Cell Biol. *6*, 665–672.

Bernardi, R., Guernah, I., Jin, D., Grisendi, S., Alimonti, A., Teruya-Feldstein, J., Cordon-Cardo, C., Simon, M.C., Rafii, S., and Pandolfi, P.P. (2006). PML inhibits HIF-1alpha translation and neoangiogenesis through repression of mTOR. Nature *442*, 779–785.

Borden, K.L., and Culjkovic, B. (2009). Perspectives in PML: a unifying framework for PML function. Front. Biosci. *14*, 497–509.

Chang, L., and Karin, M. (2001). Mammalian MAP kinase signalling cascades. Nature *410*, 37–40.

Esparis-Ogando, A., Diaz-Rodriguez, E., Montero, J.C., Yuste, L., Crespo, P., and Pandiella, A. (2002). Erk5 participates in neuregulin signal transduction and is constitutively active in breast cancer cells overexpressing ErbB2. Mol. Cell. Biol. *22*, 270–285.

Fabian, M.A., Biggs, W.H., III, Treiber, D.K., Atteridge, C.E., Azimioara, M.D., Benedetti, M.G., Carter, T.A., Ciceri, P., Edeen, P.T., Floyd, M., et al. (2005). A small molecule-kinase interaction map for clinical kinase inhibitors. Nat. Biotechnol. *23*, 329–336.

Fogal, V., Gostissa, M., Sandy, P., Zacchi, P., Sternsdorf, T., Jensen, K., Pandolfi, P.P., Will, H., Schneider, C., and Del Sal, G. (2000). Regulation of p53 activity in nuclear bodies by a specific PML isoform. EMBO J. *19*, 6185–6195.

Goldstein, D.M., Gray, N.S., and Zarrinkar, P.P. (2008). High-throughput kinase profiling as a platform for drug discovery. Nat. Rev. Drug Discov. *7*, 391–397.

Guo, A., Salomoni, P., Luo, J., Shih, A., Zhong, S., Gu, W., and Pandolfi, P.P. (2000). The function of PML in p53-dependent apoptosis. Nat. Cell Biol. *2*, 730–736.

Hayakawa, F., and Privalsky, M.L. (2004). Phosphorylation of PML by mitogen-activated protein kinases plays a key role in arsenic trioxide-mediated apoptosis. Cancer Cell *5*, 389–401.

Hayashi, M., and Lee, J.D. (2004). Role of the BMK1/ERK5 signaling pathway: lessons from knockout mice. J. Mol. Med. *82*, 800–808.

Hayashi, M., Tapping, R.I., Chao, T.H., Lo, J.F., King, C.C., Yang, Y., and Lee, J.D. (2001). BMK1 mediates growth factor-induced cell proliferation through direct cellular activation of serum and glucocorticoid-inducible kinase. J. Biol. Chem. *276*, 8631–8634.

Hayashi, M., Kim, S.W., Imanaka-Yoshida, K., Yoshida, T., Abel, E.D., Eliceiri, B., Yang, Y., Ulevitch, R.J., and Lee, J.D. (2004). Targeted deletion of BMK1/ERK5 in adult mice perturbs vascular integrity and leads to endothelial failure. J. Clin. Invest. *113*, 1138–1148.

Hayashi, M., Fearns, C., Eliceiri, B., Yang, Y., and Lee, J.D. (2005). Big mitogen-activated protein kinase 1/extracellular signal-regulated kinase 5 signaling pathway is essential for tumor-associated angiogenesis. Cancer Res. *65*, 7699–7706.

Johnson, G.L., and Lapadat, R. (2002). Mitogen-activated protein kinase pathways mediated by ERK, JNK, and p38 protein kinases. Science *298*, 1911–1912.

Kamakura, S., Moriguchi, T., and Nishida, E. (1999). Activation of the protein kinase ERK5/BMK1 by receptor tyrosine kinases. Identification and characterization of a signaling pathway to the nucleus. J. Biol. Chem. *274*, 26563–26571.

Karaman, M.W., Herrgard, S., Treiber, D.K., Gallant, P., Atteridge, C.E., Campbell, B.T., Chan, K.W., Ciceri, P., Davis, M.I., Edeen, P.T., et al. (2008). A quantitative analysis of kinase inhibitor selectivity. Nat. Biotechnol. *26*, 127–132.

Kato, Y., Kravchenko, V.V., Tapping, R.I., Han, J., Ulevitch, R.J., and Lee, J.D. (1997). BMK1/ERK5 regulates serum-induced early gene expression through transcription factor MEF2C. EMBO J. *16*, 7054–7066.

Kato, Y., Tapping, R.I., Huang, S., Watson, M.H., Ulevitch, R.J., and Lee, J.D. (1998). Bmk1/Erk5 is required for cell proliferation induced by epidermal growth factor. Nature *395*, 713–716.

Kato, Y., Zhao, M., Morikawa, A., Sugiyama, T., Chakravortty, D., Koide, N., Yoshida, T., Tapping, R.I., Yang, Y., Yokochi, T., and Lee, J.D. (2000). Big mitogen-activated kinase regulates multiple members of the MEF2 protein family. J. Biol. Chem. *275*, 18534–18540.

Kim, S.W., Chao, T.H., Xiang, R., Lo, J.F., Campbell, M.J., Fearns, C., and Lee, J.D. (2004). Tid1, the human homologue of a Drosophila tumor suppressor, reduces the malignant activity of ErbB-2 in carcinoma cells. Cancer Res. *64*, 7732–7739.

Kondoh, K., Terasawa, K., Morimoto, H., and Nishida, E. (2006). Regulation of nuclear translocation of extracellular signal-regulated kinase 5 by active nuclear import and export mechanisms. Mol. Cell. Biol. *26*, 1679–1690.

Lee, J.D., Ulevitch, R.J., and Han, J. (1995). Primary structure of BMK1: a new mammalian map kinase. Biochem. Biophys. Res. Commun. *213*, 715–724.

Mehta, P.B., Jenkins, B.L., McCarthy, L., Thilak, L., Robson, C.N., Neal, D.E., and Leung, H.Y. (2003). MEK5 overexpression is associated with metastatic prostate cancer, and stimulates proliferation, MMP-9 expression and invasion. Oncogene *22*, 1381–1389.

Mody, N., Leitch, J., Armstrong, C., Dixon, J., and Cohen, P. (2001). Effects of MAP kinase cascade inhibitors on the MKK5/ERK5 pathway. FEBS Lett. *502*, 21–24.

Patricelli, M.P., Szardenings, A.K., Liyanage, M., Nomanbhoy, T.K., Wu, M., Weissig, H., Aban, A., Chun, D., Tanner, S., and Kozarich, J.W. (2007). Functional interrogation of the kinome using nucleotide acyl phosphates. Biochemistry *46*, 350–358.

Pearson, M., and Pelicci, P.G. (2001). PML interaction with p53 and its role in apoptosis and replicative senescence. Oncogene *20*, 7250–7256.

Pearson, M., Carbone, R., Sebastiani, C., Cioce, M., Fagioli, M., Saito, S., Higashimoto, Y., Appella, E., Minucci, S., Pandolfi, P.P., and Pelicci, P.G. (2000). PML regulates p53 acetylation and premature senescence induced by oncogenic Ras. Nature *406*, 207–210.

Pearson, G., Robinson, F., Beers Gibson, T., Xu, B.E., Karandikar, M., Berman, K., and Cobb, M.H. (2001). Mitogen-activated protein (MAP) kinase pathways: regulation and physiological functions. Endocr. Rev. *22*, 153–183.

Pi, X., Garin, G., Xie, L., Zheng, Q., Wei, H., Abe, J., Yan, C., and Berk, B.C. (2005). BMK1/ERK5 is a novel regulator of angiogenesis by destabilizing hypoxia inducible factor 1alpha. Circ. Res. *96*, 1145–1151.

Raman, M., Chen, W., and Cobb, M.H. (2007). Differential regulation and properties of MAPKs. Oncogene *26*, 3100–3112.

Salomoni, P., and Pandolfi, P.P. (2002). The role of PML in tumor suppression. Cell *108*, 165–170.

Sawhney, R.S., Liu, W., and Brattain, M.G. (2009). A novel role of ERK5 in integrin-mediated cell adhesion and motility in cancer cells via Fak signaling. J. Cell. Physiol. *219*, 152–161.

Scaglioni, P.P., Yung, T.M., Cai, L.F., Erdjument-Bromage, H., Kaufman, A.J., Singh, B., Teruya-Feldstein, J., Tempst, P., and Pandolfi, P.P. (2006). A CK2-dependent mechanism for degradation of the PML tumor suppressor. Cell *126*, 269–283.

Steegmaier, M., Hoffmann, M., Baum, A., Lenart, P., Petronczki, M., Krssak, M., Gurtler, U., Garin-Chesa, P., Lieb, S., Quant, J., et al. (2007). BI 2536, a potent and selective inhibitor of polo-like kinase 1, inhibits tumor growth in vivo. Curr. Biol. *17*, 316–322.

Sticht, C., Freier, K., Knopfle, K., Flechtenmacher, C., Pungs, S., Hofele, C., Hahn, M., Joos, S., and Lichter, P. (2008). Activation of MAP kinase signaling through ERK5 but not ERK1 expression is associated with lymph node metastases in oral squamous cell carcinoma (OSCC). Neoplasia *10*, 462–470.

Trotman, L.C., Alimonti, A., Scaglioni, P.P., Koutcher, J.A., Cordon-Cardo, C., and Pandolfi, P.P. (2006). Identification of a tumour suppressor network opposing nuclear Akt function. Nature *441*, 523–527.

Weldon, C.B., Scandurro, A.B., Rolfe, K.W., Clayton, J.L., Elliott, S., Butler, N.N., Melnik, L.I., Alam, J., McLachlan, J.A., Jaffe, B.M., et al. (2002). Identification of mitogen-activated protein kinase kinase as a chemoresistant pathway in MCF-7 cells by using gene expression microarray. Surgery *132*, 293–301.

Yan, C., Luo, H., Lee, J.D., Abe, J., and Berk, B.C. (2001). Molecular cloning of mouse ERK5/BMK1 splice variants and characterization of ERK5 functional domains. J. Biol. Chem. *276*, 10870–10878.

Zhou, C., Nitschke, A.M., Xiong, W., Zhang, Q., Tang, Y., Bloch, M., Elliott, S., Zhu, Y., Bazzone, L., Yu, D., et al. (2008). Proteomic analysis of tumor necrosis factor-alpha resistant human breast cancer cells reveals a MEK5/Erk5-mediated epithelial-mesenchymal transition phenotype. Breast Cancer Res. *10*, R105.